

3D facial morphometry in Italian patients affected by Aicardi syndrome.

Silvia Masnada^{1*}, Daniele Gibelli^{2*}, Claudia Dolci², Valentina De Giorgis³, Annalisa Cappella²,

Pierangelo Veggiotti^{1,4§}, Chiarella Sforza^{2§}

and *The Italian Aicardi study group*: Renato Borgatti, Francesca La Briola, Laura Canafoglia, Alberto Danieli, Francesca Darra, Valentina De Giorgis, Tiziana Granata, Silvia Masnada, Romina Romaniello, Carlotta Spagnoli, Pierangelo Veggiotti, Aglaia Vignoli.

*Drs Masnada and Gibelli should be considered joint first author

§ Drs Sforza and Veggiotti should be considered joint senior author

¹Department of Child Neurology, V. Buzzi Children's Hospital, University of Milan, Italy

²Functional Anatomy Research Center (FARC), Laboratorio di Anatomia Funzionale dell'Apparato Stomatognatico (LAFAS), Dipartimento di Scienze Biomediche per la Salute, Università degli Studi di Milano, Milano, Italy

³IRCCS Mondino Foundation, Pavia, Italy,

⁴Department of Biomedical and Clinical Sciences, L. Sacco, University of Milan, Italy

Silvia.Masnada@asst-fbf-sacco.it (ORCID 0000-0003-3850-8849), Daniele.Gibelli@unimi.it (ORCID 0000-0002-9591-1047), Claudia.Dolci@unimi.it (ORCID 0000-0002-3060-4097), Valentina.Degiorgis@mondino.it (ORCID 0000-0002-5828-7070), Annalisa.Cappella@unimi.it (ORCID 0000-0002-4527-4203), Pierangelo.Veggiotti@unimi.it (ORCID 0000-0003-2851-3441), Chiarella.Sforza@unimi.it (ORCID 0000-0001-6532-6464)

Original article #20-0389 submitted to the *American Journal of Medical Genetics* on April 15th 2020
– first revision June 9th, 2020

Number of Figures: 2

Number of Tables: 2

Running title: Facial morphometry in Aicardi syndrome.

Corresponding author:

Prof. Chiarella Sforza

Department of Biomedical Sciences for Health

Università degli Studi di Milano

via Mangiagalli 31

20133 Milano - Italy.

Phone: +39 0250315385 - Fax: +39 0250315387

e-mail: chiarella.sforza@unimi.it

3D facial morphometry in Italian patients affected by Aicardi syndrome.

Abstract

Aicardi syndrome (AIC) is a rare congenital neurodevelopmental disorder of unknown etiology, that affects almost exclusively females, originally characterized by corpus callosum agenesis, chorioretinal lacunae and infantile spasms. The current diagnostic criteria also include qualitative facial features (prominent premaxilla, upturned nasal tip, decreased nasal bridge angle, sparse lateral eyebrows, microphthalmia) that still need quantification. We performed a 3D photogrammetric assessment of 11 Italian females, age 7-32 years, who satisfied AIC criteria. Linear distances and angles were computed from soft-tissue facial landmarks coordinates. Z-score values were calculated using data of 850 healthy reference females matched for age and compared by Mann-Whitney test ($p < 0.01$). Patients showed a shorter philtrum and right side orbital height (mean z-scores: -1.7, -0.9), shorter superior, middle and inferior facial depths (mean z-scores: -1.3, -2.2, -2.3), and a smaller length of mandibular ramus (mean z-score: -2.1); conversely, they showed larger nasal and lower facial widths, and lower facial convexity (mean z-scores: 1.7, 1.4, 2.4). The inclinations of the orbit versus the true horizontal were increased bilaterally (mean z-scores: 1.8, 1.1). Some common facial abnormalities were quantified in AIC patients using a non-invasive instrument. They may help clinicians in performing a definite AIC diagnosis in atypical or doubt cases.

Key words: Aicardi syndrome; face; 3D; stereophotogrammetry; neurology.

Introduction

Aicardi syndrome (AIC; OMIM %304,050) is a rare congenital condition, described for the first time in its classical triad, corpus callosum agenesis, chorioretinal lacunae and infantile spasms, by Jean Aicardi in 1965 and currently defined on the basis of the Sutton modified diagnostic criteria (Aicardi et al., 1965; Sutton et al., 2005; Wong and Sutton, 2018). Patients are almost exclusively girls or boys with Klinefelter syndrome, and the rate of incidence of AIC ranges between 1:93.000 and 1:167.000 live births, with an estimated worldwide prevalence over 4000 (Kroner et al., 2008).

The increasing number of patients cohorts and single case studies reported in literature allowed a better definition of the phenotype: chorioretinal lacunae, considered pathognomonic, are round, depigmented areas of the retinal pigment epithelium underlying choroid with variably dense pigmentation at their borders, frequently associated with other ocular abnormalities such as coloboma, microphthalmos and cataracts. Infantile spasms are the most characteristic type of seizures, but also other types of seizures, such as focal, tonic, generalized tonic-clonic, myoclonic, atonic seizures and status epilepticus, are reported (Glasmacher et al., 2007), together with severe intellectual disability and global developmental alterations (Kroner et al., 2008). Corpus callosum agenesis is almost never an isolated finding, but frequently associated with a complex brain malformation consisting of polymicrogyria, interhemispheric and/ or choroid plexus cysts, nodular heterotopias, and posterior fossa abnormalities (Hopkins et al., 2008).

Extensive genetic studies carried on so far by several international research groups, such as skewed X-inactivation analysis (Eble et al., 2009), candidate genes studies (Van den Veyver et al., 2004), methylation array (Piras et al., 2017), exome and genome sequencing (Lund et al., 2016; Wang et al., 2009; Wong and Sutton, 2018), failed to solve the AIC etiology. Considering the absence of a genetic etiology, AIC diagnosis is still a challenge because diagnostic criteria are based only on clinical and radiological features (Aicardi, 2005; Sutton et al., 2005). Examining 40 child and adolescent girls with AIC, Sutton and colleagues noticed some consistent facial features: prominent premaxilla, upturned nasal tip, decreased angle of the nasal bridge, and sparse lateral eyebrows, in over half of the patients, and proposed their inclusion in the diagnostic criteria (Sutton et al., 2005). More recently, Wong and

Sutton (2018) included microphthalmia in the morphological description of patients, often with an asymmetric presentation that involved the right eye more than the left.

Actually, most of those facial features were only qualitatively described (Sutton et al., 2005; Wong and Sutton, 2018), and they still need quantification. To the best of our knowledge, no other studies presented detailed measurements about the facial characteristics of patients with AIC, that were even reported to be subtle and too unspecific for diagnostic purposes (Lund et al., 2015).

Currently, the three-dimensional (3D) characteristics of facial soft tissues can be quantitatively recorded and analyzed using several computerized instruments, and a variety of studies have widely delineated that different syndromes possess a typical facial phenotype that can drive clinicians toward the diagnosis (Dolci et al., 2018; Kruszka et al., 2017, 2018; Pucciarelli et al., 2017a, b; Sforza et al., 2004, 2012, 2015). In particular, the facial characteristics of patients with several syndromes with intellectual disability were successfully described and quantified, and the same approach may be applied to the study of patients with AIC.

For instance, when compared to healthy subjects of the same sex, age and ethnicity, Italian patients with Down syndrome showed a reduced facial size, underdeveloped maxillary and mandibular regions with smaller soft-tissue facial areas and volumes (ears, eyes, nose, lower lip), a prominent forehead, a depressed nasal bridge (Sforza et al., 2004, 2012, 2015). Northern Sudanese and Asian patients with Down syndrome showed similar specific facial features but the differences relative to their reference healthy subjects were smaller than those seen in the Italian patients (Kruszka et al., 2017; Sforza et al., 2015).

Patients with Glut1 deficiency syndrome (Glut1-DS), a disorder characterized by an impaired transport of glucose across the blood brain barrier, showed peculiar soft-tissue facial features in the mandible (more anterior chin, longer mandibular body coupled with shorter mandibular rami, and reduced gonial angles) and eyes (reduced intercanthal distance, smaller and down-slanted palpebral fissures) (Pucciarelli et al., 2017a).

A quantitative analysis of the phenotype of patients with Williams–Beuren syndrome, a microdeletion syndrome in 7q11.23, reported significant alterations in size, shape and position of nose (short with a

long philtrum), mouth (thick lip vermillion, wide mouth), and ear lobes (increased). Ethnic-related characteristics were also found (Kruszka et al., 2018).

Considering the approach used in the prior studies for the quantitative description of the facial phenotype of these syndromes, and taking the first Sutton observations into account, our aim was to perform a 3D stereophotogrammetric assessment in a cohort of Italian patients with AIC in order to investigate if a specific facial phenotype could be identified to help the clinicians in the diagnosis.

Materials and Methods

Recruitment of subjects and 3D facial acquisition

Eleven female northern Italian patients aged between 7 and 32 years (mean age: 17.5, SD: 8.2 years; median age: 16, interquartile range: 12-23 years) who satisfied AIC Sutton criteria were included in the study (Sutton et al., 2005). An informed consent was signed by parents of everyone, in accordance with the Declaration of Helsinki. The experimental project was approved by the local university ethical committee (26.03.14; n° 92/14).

Patients underwent 3D facial photographs through stereophotogrammetry (VECTRA® M3: Canfield Scientific, Inc., Fairfield, NJ, USA). The instrument comprises three pods, each with one high resolution black-and-white camera and one color camera; the cameras image the facial soft tissues simultaneously from different points of view with a single shot lasting less than 2 ms, and a digital 3D model with a geometric resolution of 1.2 mm is provided. A previous calibration of the instrument is performed to provide 3D metrical data independent from head position and to correct optical and electronical distortion of the images. The scanning procedure is not invasive and without biological risks, the only disturb may be given by the cameras' flashes. Each subject was imaged in neutral seated position, with a neutral facial expression (no grimace, smile, pursed lips) and close mouth compatibly with her collaboration. Multiple 3D photographs were made when necessary and possible; five to eight photographs were collected in most patients, with a maximum of 10 facial scans.

Each 3D facial model was elaborated by VAM® software (Canfield Scientific, Inc., Fairfield, NJ, USA). The model comprises a polygon mesh obtained by matching corresponding points in the greyscale images of the three pods, and a color texture obtained from the color cameras. The texture information is added to the 3D model and a photorealistic 3D image is provided that can be enlarged, rotated, and shifted for a full ear-to-ear and forehead-to-neck view (De Menezes et al., 2010). In total, 18 linear measurements and 14 angles were automatically calculated through Faces software (developed by our laboratory specifically for the extraction of metrical parameters from coordinates), after the selection of 50 facial landmarks defined according to Farkas (De Menezes et al., 2009;

Farkas, 1994). Repeatability and accuracy of data collection procedure were verified (De Menezes et al., 2010).

The selection of measurements was done according to our previous studies on facial morphological alterations in syndromes involving the central nervous system (Pucciarelli et al. 2017a,b, 2019; Sforza et al., 2004, 2012, 2015) as well as considering the facial morphological features reported by Sutton et al. (2005) and by Wong and Sutton (2018). Figure 1 shows the positions of the subset of landmarks actually used for the current calculation of distances and angles, that are listed in Table 1.

For each patient, a group of control girls/ women of the same age and ethnicity who underwent the same facial 3D analysis, was selected from the database of the laboratory to serve as a reference group. In total, 850 healthy subjects were analyzed; each age-related reference group comprised a minimum of 29 subjects. The control subjects came from the general population, and were free from pathological conditions affecting the head and the face, without a history of facial trauma, maxillofacial surgery, craniofacial syndromes or deformities, and neurological impairments.

Additionally, the main facial characteristics listed by Sutton et al. (2005), together with some companion features, were analyzed qualitatively in the current patients by three dysmorphologists who examined the 3D facial reproductions of the 11 patients.

Statistical analysis

The comparison between patients and the corresponding group of healthy subjects was performed by calculating z-scores:

$$z\text{-score} = (x - \mu) / \sigma$$

where x is the value of each measurement calculated in the patient, and μ (mean) and σ (standard deviation) are the relevant values computed on the healthy subjects. The smaller the z-score in absolute value, the closer the patient values to the reference ones.

Possible statistically significant differences in z-score for each measurement between patients and control subjects were assessed through Mann-Whitney test ($p < 0.01$).

Results

All the patients with AIC satisfied the Sutton diagnostic criteria; ten AIC patients presented the classical diagnostic triade: chorioretinal lacunae, corpus callosum agenesis and infantile spasms; only one patient lacked chorioretinal lacunae but the diagnosis is strongly suggestive because she satisfied the Sutton criteria considering the presence of two classical features (corpus callosum agenesis and infantile spasms), three major features (cortical malformations, particularly polymicrogyria, periventricular heterotopia, choroid plexus cysts) and one supporting feature (upturned nasal tip sparse lateral eyebrows) All the patients displayed infantile spasms at their epilepsy onset, with a severe derangement of EEG trace and multifocal epileptiform discharges, six of them with a definite hypsarrhythmic pattern and in one case a suppression burst pattern. All patients developed a drug resistant epilepsy, with multiple types of seizures, mostly spasms and focal seizures, but also atonic, myoclonic seizures and status epilepticus were reported.

Table 2 reports the occurrence of the main morphological facial features observed in the patients. While the presence of sparse lateral eyebrows was in good accord with previous reports (Sutton et al., 2005), most of our patients did not show a prominent premaxilla (7/11) and/ or an upturned nasal tip. In contrast, a reduced lower lip/ chin was observed in 3/11 girls: in two of them this feature was coupled with an apparently prominent premaxilla. Only 2/11 girls were imaged with a closed mouth, while 7/11 had opened lips: this condition could negatively affect the subsequent facial measurements of the labial area.

Descriptive statistics of the z-scores for each measurement are shown in Table 1. Among linear distances, eight measurements showed a statistically significant difference between patients and healthy subjects, together with five angles, with an average deviation from the mean reference values ranging between 0.9 and 2.4 standard deviations (Fig. 2a, b). In detail, all patients showed a shorter labial philtrum (mean z-score: -1.7), shorter superior, middle and inferior facial depths (mean z-scores: -1.3, -2.2 and -2.3, respectively), and a smaller length of mandibular ramus (mean z-score: -2.1). Orbital height was significantly reduced but only on the right side (mean z-score: -0.9).

The patients showed higher values than control subjects in nasal and lower facial widths (mean z-scores: 1.7, 1.4, respectively). Among the angles, upper, middle and lower facial convexities were significantly increased in patients (mean z-scores: 1.7, 1.4, 2.4, respectively). On both sides, the inclinations of the orbit versus the true horizontal were increased (the vertical projections of the orbitale superius and orbitale landmarks were further away one from the other).

Overall, most of these features were found in all (superior, middle and inferior facial depths, upper and lower facial convexities, mandibular ramus length, nasal width, labial philtrum, right side inclination of the orbit versus the true horizontal) or almost all (middle facial convexity 10/11, lower facial width 9/11, right side orbital height 9/11, left side inclination of the orbit versus the true horizontal 9/11) analyzed patients with AIC, independently from age.

Discussion

Up to date AIC diagnosis is based on clinical and neuroradiological features. Over the years, patients without one out of the three classical criteria, namely without callosal agenesis (Iturralde et al., 2006) or spasms (Prats Vinas et al., 2005) or chorioretinal lacunae (Sutton et al., 2005), and atypical cases (Lee et al., 2004) have been increasingly described in literature, making a challenge to perform a definite diagnosis. In absence of genetic or biological markers, to find more definite parameters in order to reinforce the diagnosis becomes needful. To allow a better description of the disease, a quantitative approach should be applied, thus giving more value and specificity to diagnosis (Lund et al., 2015).

To the scope, 3D facial surface analysis represents a valuable method for extracting several linear and angular measurements, useful for a comparison with control subjects. As previously demonstrated in other studies, a 3D morphometric analysis proved itself powerful in the identification of specific facial features of definite syndromes (Dolci et al., 2018; Kruszka et al., 2017, 2018; Pucciarelli et al., 2017a, b, 2019; Sforza et al., 2004, 2012, 2015). In addition, stereophotogrammetry has an acquisition time lower than 2 ms, which allows to perform a 3D facial scan even in individuals with special needs, such as patients with spasms or very active persons, as in the current study. Nonetheless, some technical limitations prevented to assess all facial structures with the same precision: in particular, due to the reduced cooperation of the patients, we were not able to correctly record the ear region because of hairs. Also, most of the patients did not close their mouth during the 3D photographic records, and, notwithstanding the multiple scans, data obtained in the labial area should be considered with caution. As far as ears are concerned, previous reports showed a significantly increased ear length (Sutton et al., 2005), that should be analyzed with an alternative protocol.

Despite the clinical and neuroradiological variability of the syndrome, our quantitative approach allowed us to identify some facial features common to all patients with AIC who, in comparison to reference subjects, had an overall flatter face in the anterior-posterior direction with shorter philtrum and mandibular ramus, and wider nose. Also, more than 80% of patients showed a wider lower face and altered orbital inclinations.

Lack of knowledge regarding the etiology of the disease does not help in understanding these observations; moreover, the effects of adrenocorticotrophic hormone (ACTH) or steroid therapies usually used for infantile spasms, cannot be excluded in influencing the facial features observed. For instance, lower facial width may be influenced by the deposition of adipose tissue. At the same time, a wider lower face and nose, together with a shorter mandibular ramus and an increased lower facial convexity, were recently described in children affected by Spinal muscular atrophy type II (SMA), a severe muscular disease with hypotonia, areflexia, weakness and respiratory impairment (Pucciarelli et al., 2019). The alterations were tentatively explained by the reduced muscular activity.

On the other hand, clinical data about facial morphology previously reported by literature were not fully confirmed by 3D analysis: differences between our patients and control subjects were not detected for what concerns $sl-n-sn$ (maxillary prominence angle), $prn-sn-ls$ (nasolabial angle), and $prn-n-sn$ (nasal convexity). These three angles were selected to measure nasal prominence (reduced convexity with an anterior-positioned sn landmark), and to detect the prominence of the premaxilla per se (increased nasolabial angle; Allanson et al., 2009), or relatively to the mandible (maxillary prominence angle). Even if a normal nasolabial angle could result from a combined modification of nose and upper lip positions, we could not quantitatively confirm the prominent premaxilla and upturned nasal tip detected in the previous study by Sutton and colleagues (Sutton et al., 2005). As this clinical description may not necessarily be caused by an increase in size of the premaxilla, but be the result of a combination of factors, we can tentatively combine our patients with a prominent premaxilla and upturned nasal tip with those with a relatively reduced lower lip and chin area. Thus, a total of six patients (55%) might be classified in (at least) partial agreement with Sutton et al. (2005) who reported the feature in 66% of their 40 patients, and of Lund et al. (2015) who described this condition in four out of five patients.

It has to be mentioned that Sutton et al. (2005) measured patients aged up to 16 years, while our group encompassed patients aged 7 to 32 years: even if we did not observe specific age-related trends in facial morphometry, the reduced sample size impedes speculations. In contrast, we confirmed the presence of sparse lateral eyebrows in about half of the patients (43% in Sutton et al., 2005), the reduced philtrum length (100% of patients with negative z-score; current mean z-score: -1.7, Sutton -

1.9) and a trend of modifications in the outer canthal (reduced, current mean z -score: -0.1, Sutton -0.7) and inter canthal (increased, current mean z-score:1.0, Sutton 0.2) distances (Sutton et al., 2005).

In the orbital area, a significant reduction of right side orbital height was found: 90% of the patients had a negative z-score, thus confirming the microphthalmia (25% of patients according to Sutton et al., 2005, 2 out of 6 according to Lund et al., 2015), and its asymmetric presentation (Wong and Sutton, 2018). No significant differences were observed for palpebral fissure widths but some patients had reduced measurement (six, both sides; one, right side only). The patients also showed a significant increment in the inclinations of the orbits versus the true horizontal (100%, right side, 80%, left side), a modification seen also in other neurodevelopmental disorders (Pucciarelli et al., 2019).

Among the limits of the study there is the number of analyzed patients. Even if the rarity of the disorder justifies the small sample size, further 3D morphometric analyses including patients with AIC syndrome should be planned, extending the cohort in study, increasing the power of the statistical analysis and better supporting our findings. Considering the reduced number of patients with AIC, international collaborations appear as the best opportunity to collect an adequate sample size, as well as to verify possible differences in phenotype among ethnicities (Kruszka et al., 2017, 2018; Sforza et al., 2015). At the moment, facial features seem to have been reported in European/ Northern American patients only (Lund et al., 2015; Sutton et al., 2005; current study), and any hypotheses is premature.

Other limitations relative to some facial structures are intrinsic in the measurement protocol, as detailed before.

The detection of similar facial measurements in all the AIC patients, if confirmed in larger cohorts, will have significant applications in clinical practice. From one side, it will help clinicians in performing a definite AIC diagnosis when classifying atypical or doubt cases. Moreover, it will help researchers in performing genetic analysis in more selected and homogeneous cases, opening the way to new potential clarification of the etiology of the syndrome (Wong and Sutton, 2018).

In conclusion, the present article first provided quantitative data about facial morphology of patients affected by AIC through 3D surface facial analysis. Results will be useful to improve our knowledge of this severe and incompletely explored pathology.

Acknowledgments

Conflict of interest - The authors have no conflict of interest to declare.

Role of the funding source - No funding sources.

Ethics - The investigation complies with the principles stated in the Declaration of Helsinki “Ethical Principles for Medical Research Involving ‘Human Subjects’”. Ethical approval obtained by the ethical committee of Università degli Studi di Milano, Milan, Italy (26.03.14; n° 92/14).

Author contributions

Silvia Masnada: study design, data collection and analysis, drafting the paper, final approval of the submission.

Daniele Gibelli: study design, data collection and analysis, drafting the paper, final approval of the submission.

Claudia Dolci: data collection, analysis and interpretation, revising the papers’ draft for important intellectual concepts, final approval of the submission.

Valentina De Giorgis: data collection and analysis, revising the papers’ draft for important intellectual concepts, final approval of the submission.

Annalisa Cappella: data collection and interpretation, revising the papers’ draft for important intellectual concepts, final approval of the submission.

Pierangelo Veggiotti: study design, data interpretation, revising the papers’ draft for important intellectual concepts, final approval of the submission.

Chiarella Sforza: study design, data analysis and interpretation, revising the papers’ draft for important intellectual concepts, final approval of the submission.

Data availability statement - The data that support the findings of this study are available on request from the corresponding author. The data are not publicly available due to privacy and ethical restrictions.

References

- Aicardi, J. (2005). Aicardi syndrome. *Brain & Development*, 27(3), 164-171.
Doi:<https://doi.org/10.1016/j.braindev.2003.11.011>
- Aicardi, J., Lefebvre, J., & Leriche-Koechlin, A. (1965). A new syndrome: spasms in flexion, callosal, agenesis, ocular abnormalities. *Electroencephalogram and Clinical Neurophysiology*, 19, 609-610.
- Allanson, J.E., Cunniff, C., Hoyme, H.E., McGaughan, J., Muenke, M. & Neri, G. (2009). Elements of morphology: standard terminology for the head and face. *American Journal of Medical Genetics Part A*, 149A(1), 6-28. doi: 10.1002/ajmg.a.32612

- De Menezes, M., Rosati, R., Allievi, C., & Sforza, C. (2009). A photographic system for three-dimensional study of facial morphology. *Angle Orthodontist*, 79(6), 1070-1077. doi: <https://doi.org/10.2319/111008-570>
- De Menezes, M., Rosati, R., Ferrario, V.F., & Sforza, C. (2010). Accuracy and reproducibility of a 3-dimensional stereophotogrammetric imaging system. *Journal of Oral and Maxillofacial Surgery*, 68(9), 2129-2135. doi: <https://doi.org/10.1016/j.joms.2009.09.036>
- Dolci, C., Pucciarelli, V., Gibelli, D.M., Codari, M., Marelli, S., Trifiro, G., Pini, A., & Sforza, C. (2018). The face in Marfan syndrome: A 3D quantitative approach for a better definition of dysmorphic features. *Clinical Anatomy*, 31(3), 380-386. doi: <https://doi.org/10.1002/ca.23034>
- Eble, T.N., Sutton, V.R., Sangi-Haghepykar, H., Wang, X., Jin, W., Lewis, R.A., Fang, P., & Van den Veyver, I.B. (2009). Non-random X chromosome inactivation in Aicardi syndrome. *Human Genetics*, 125(2), 211-216. doi: <https://dx.doi.org/10.1007%2Fs00439-008-0615-4>
- Farkas, L.G. (1994) *Anthropometry of the head and face*, New York, NY: Raven Press.
- Glasmacher, M.A., Sutton, V.R., Hopkins, B., Eble, T., Lewis, R.A., Park Parsons D., & Van den Veyver, I.B. (2007) Phenotype and management of Aicardi syndrome: new findings from a survey of 69 children. *Journal of Child Neurology*, 22(2), 176-184. doi: <https://doi.org/10.1177%2F0883073807300298>
- Hopkins, B., Sutton, V.R., Lewis, R.A., Van den Veyver, I., & Clark, G. (2008) Neuroimaging aspects of Aicardi syndrome. *American Journal of Medical Genetics Part A*, 146A(22), 2871-2878. Doi: <https://doi.org/10.1002/ajmg.a.32537>
- Iturralde, D., Meyerle, C.B., & Yannuzzi, L.A. (2006) Aicardi syndrome: chorioretinal lacunae without corpus callosum agenesis. *Retina*, 26(8), 977-978. doi: 10.1097/01.iae.0000224937.78389.15
- Kroner, B.L., Preiss, L.R., Ardini, M.A., & Gaillard, W.D. (2008) New incidence, prevalence, and survival of Aicardi syndrome from 408 cases. *Journal of Child Neurology*, 23(5), 531-535. doi: 10.1177/0883073807309782.
- Kruszka, P., Porras, A.R., Sobering, A.K., Ikolo, F.A., La Qua, S., Shotelersuk, V., Chung, B.H., Mok, G.T., Uwineza, A., Mutesa, L., Moresco, A., Obregon, M.G., Sokunbi, O.J., Kalu, N., Joseph, D.A., Ikebudu, D., Ugwu, C.E., Okoromah, C.A., Addissie, Y.A., Pardo, K.L., Brough, J.J., Lee, N.C., Girisha, K.M., Patil S.J., Ng, I.S., Min, B.C., Jamuar, S.S., Tibrewal, S., Wallang, B., Ganesh, S., Sirisena, N.D., Dissanayake, V.H., Paththinige, C.S., Prabodha, L.B., Richieri-Costa, A., Muthukumarasamy, P., Thong, M.K., Jones, K.L., Abdul-Rahman, O.A., Ekure, E.N., Adeyemo, A.A., Summar, M., Linguraru, M.G., Muenke, M. (2017) Down syndrome in diverse populations. *American Journal of Medical Genetics Part A*, 173A(1), 42-53. doi: 10.1002/ajmg.a.38043.
- Kruszka, P., Porras, A.R., de Souza, D.H., Moresco, A., Huckstadt, V., Gill, A.D., Boyle, A.P., Hu, T., Addissie, Y.A., Mok, G.T.K., Tekendo-Ngongang, C., Fieggen, K., Prijoles, E.J., Tanpaiboon,

- P., Honey, E., Luk, H.M., Lo, I.F.M., Thong, M.K., Muthukumarasamy, P., Jones, K.L., Belhassan, K., Ouldim, K., El Bouchikhi, I., Bouguenouch, L., Shukla, A., Girisha, K.M., Sirisena, N.D., Dissanayake, V.H.W., Paththinige, C.S., Mishra, R., Kisling, M.S., Ferreira, C.R., de Herreros, M.B., Lee, N.C., Jamuar, S.S., Lai, A., Tan, E.S., Ying Lim, J., Wen-Min, C.B., Gupta, N., Lotz-Esquivel, S., Badilla-Porras, R., Hussen, D.F., El Ruby, M.O., Ashaat, E.A., Patil, S.J., Dowsett, L., Eaton, A., Innes, A.M., Shotelersuk, V., Badoe, Ě., Wonkam, A., Obregon, M.G., Chung, B.H.Y., Trubnykova, M., La Serna, J., Gallardo Jugo, B.E., Chávez Pastor, M., Abarca Barriga, H.H., Megarbane, A., Kozel, B.A., van Haelst, M.M., Stevenson, R.E., Summar, M., Adeyemo, A.A., Morris, C.A., Moretti-Ferreira, D., Lingurar, M.G., Muenke, M. (2018) Williams-Beuren syndrome in diverse populations. *American Journal of Medical Genetics Part A*, 176A(5): 1128-1136. doi: 10.1002/ajmg.a.38672.
- Lee, S.W., Kim, K.S., Cho, S.M., & Lee, S.J. (2004) An atypical case of Aicardi syndrome with favorable outcome. *Korean Journal of Ophthalmology*, 18(1), 79-83. doi: 10.3341/kjo.2004.18.1.79
- Lund, C., Bjørnvold, M., Tuft, M., Kostov, H., Røsby, O. & Selmer, K.K. (2015) Aicardi Syndrome: An Epidemiologic and Clinical Study in Norway, *Pediatric Neurology*, 52(2), 182-186.e3, doi.org/10.1016/j.pediatrneurol.2014.10.022.
- Lund, C., Striano, P., Sorte, H.S., Parisi, P., Iacomino, M., Sheng, Y., Vigeland, M.D., Oye, A.M., Moller, R.S., Selmer, K.K., & Zara, F. (2016). Exome Sequencing Fails to Identify the Genetic Cause of Aicardi Syndrome. *Molecular Syndromology*, 7(4), 234-238. doi: 10.1159/000448367
- Piras, I.S., Mills, G., Llaci, L., Naymik, M., Ramsey, K., Belnap, N., Balak, C.D., Jepsen, W.M., Szelinger, S., Siniard, A.L., Lewis, C.R., LaFleur, M., Richholt, R.F., De Both, M.D., Avela, K., Rangasamy, S., Craig, D.W., Narayanan, V., Jarvela, I., Huentelman, M.J., & Schrauwen, I. (2017). Exploring genome-wide DNA methylation patterns in Aicardi syndrome. *Epigenomics*, 9(11), 1373-1386. doi: 10.2217/epi-2017-0060.
- Prats Vinas, J.M., Martinez Gonzalez, M.J., Garcia Ribes, A., Martinez Gonzalez, S., & Martinez Fernandez, R. (2005). Callosal agenesis, chorioretinal lacunae, absence of infantile spasms, and normal development: Aicardi syndrome without epilepsy? *Developmental Medicine & Child Neurology*, 47(6), 419-420. doi: 10.1017/s0012162205000812
- Pucciarelli, V., Bertoli, S., Codari, M., De Amicis, R., De Giorgis, V., Battezzati, A., Veggiotti, P., & Sforza, C. (2017a). The face of Glut1-DS patients: A 3D Craniofacial Morphometric Analysis. *Clinical Anatomy*, 30(5), 644-652. doi: 10.1002/ca.22890. doi: 10.1002/ca.22890.
- Pucciarelli, V., Bertoli, S., Codari, M., Veggiotti, P., Battezzati, A., & Sforza, C. (2017b). Facial Evaluation in Holoprosencephaly. *Journal of Craniofacial Surgery*, 28(1), e22-e28. doi: 10.1097/SCS.00000000000003171
- Pucciarelli, V., Gibelli, D., Mastella, C., Bertoli, S., Alberti, K., De Amicis, R., Codari, M., Dolci, C., Battezzati, A., Baranello, G., & Sforza, C. (2019). 3D Facial morphology in children affected by

- spinal muscular atrophy type 2 (SMAII). *European Journal of Orthodontics*, doi: 10.1093/ejo/cjz071.
- Sforza, C., Dellavia, C., Zanotti, G., Tartaglia, G.M., Ferrario, V.F. (2004). Soft tissue facial areas and volumes in subjects with Down syndrome. *American Journal of Medical Genetics Part A*, 130A(3): 234-239. DOI: 10.1002/ajmg.a.30253
- Sforza, C., Dellavia, C., Allievi, C., Tommasi, D.G., Ferrario, V.F. (2012). Anthropometric indices of facial features in Down's syndrome subjects. In: V.R. Preedy (Ed.). *Handbook of Anthropometry: Physical Measures of Human Form in Health and Disease.*, Springer Science+Business Media, LLC; Chapter 98, pp. 1603-1618. doi: 10.1007/978-1-4419-1788-1_98.
- Sforza, C., Dolci, C., Dellavia, C., Gibelli, D.M., Tartaglia, G.M., Elamin, F. (2015). Abnormal variations in the facial soft tissues of individuals with Down Syndrome: Sudan versus Italy. *The Cleft Palate-Craniofacial Journal*, 52(5):588-96. doi: 10.1597/14-082.
- Sutton, V.R., Hopkins, B.J., Eble, T.N., Gambhir, N., Lewis, R.A., & Van den Veyver, I.B. (2005). Facial and physical features of Aicardi syndrome: infants to teenagers. *American Journal of Medical Genetics Part A*, 138A(3), 254-258. doi: 10.1002/ajmg.a.30963
- Van den Veyver, I.B., Panichkul, P.P., Antalffy, B.A., Sun, Y., Hunter, J.V., & Armstrong, D.D. (2004). Presence of filamin in the astrocytic inclusions of Aicardi syndrome. *Pediatric Neurology*, 30(1), 7-15. doi: 10.1016/s0887-8994(03)00311-4
- Wang, X., Sutton, V.R., Eble, T.N., Lewis, R.A., Gunaratne, P., Patel, A., & Van den Veyver, I.B. (2009). A genome-wide screen for copy number alterations in Aicardi syndrome. *American Journal of Medical Genetics Part A*, 149A(10), 2113-2121. doi: 10.1002/ajmg.a.32976
- Wong, B.K.Y., & Sutton, V.R. (2018). Aicardi syndrome, an unsolved mystery: Review of diagnostic features, previous attempts, and future opportunities for genetic examination. *American Journal of Medical Genetics Part C Seminars in Medical Genetics*, 178C(4), 423–431. doi: 10.1002/ajmg.c.31658

Figure Legends

Figure 1: Facial landmarks used for the automatic calculation of distances and angles. Unpaired (midline): t, trichion; n, nasion; prn, pronasale; sn, subnasale; ls, labiale superior; li, labiale inferior; sl, sublabiale; pg, pogonion; paired (left and right side): ex, exocanthion; en, endocanthion; os, orbitale superior; or, orbitale; al, alare; t, tragus; zy, zygion; go, gonion.

Figure 2a,b: Measurements showing statistically significant differences between patients and healthy subjects: red lines show linear distances that are smaller in patients than in healthy subjects, blue lines show linear distances that are longer in patients than in healthy subjects (only distances that differ more than ± 1 z-score are depicted). The blue triangle shows the only sagittal plane angle larger than 2 z-scores.

Table 1. Definition of the measurements, descriptive statistics of the z-scores and relevant p-values (Mann-Whitney test).

			Definition	z-score	SD	p	
Linear distances	Horizontal	$ex_r - ex_l$	Outer canthal distance	-0.1	1.5	0.685	
		$en_r - en_l$	Inter canthal distance	1.0	1.7	0.076	
		$en_r - ex_r$	Right palpebral fissure width	0.0	1.1	0.247	
		$en_l - ex_l$	Left palpebral fissure width	0.2	1.0	0.699	
		$t_r - t_l$	Middle facial width	0.1	1.6	0.699	
		$go_r - go_l$	Lower facial width	1.4	1.2	0.007	
		$zy_r - zy_l$	Facial width	0.6	1.4	0.699	
		$al_r - al_l$	Nasal width	1.7	1.3	<0.001	
	Vertical	$tr - n$	Forehead length	-0.5	1.6	0.054	
		$n - sn$	Nasal height	0.3	0.9	0.430	
		$sn - ls$	Philtrum length	-1.7	1.2	<0.001	
		$os_r - or_r$	Right orbital height	-0.9	1.1	0.010	
		$os_l - or_l$	Left orbital height	-0.3	1.1	0.300	
	Sagittal	$n - t_m$	Upper facial depth	-1.3	0.7	<0.001	
		$sn - t_m$	Midfacial depth	-2.2	1.1	<0.001	
		$pg - t_m$	Lower facial depth	-2.3	1.5	<0.001	
		$pg - go_m$	Mandibular body length	0.5	1.1	0.247	
		$t_m - go_m$	Mandibular ramus length	-2.1	1.4	<0.001	
	Angles	Horizontal	$t_r - n - t_l$	Upper facial convexity	1.3	1.4	0.010
			$t_r - prn - t_l$	Middle facial convexity	1.9	2.1	<0.001
$t_r - pg - t_l$			Lower facial convexity	2.4	2.5	0.001	
$go_r - pg - go_l$			Mandibular convexity	0.1	1.1	0.700	
$t_r - go_r - pg$			Right gonial angle	-0.4	2.4	0.700	
$t_l - go_l - pg$			Left gonial angle	-0.4	1.9	0.699	
$al_r - prn - al_l$			Alar slope angle	0.2	0.6	0.247	
Vertical		$os_r - or_r$ vs TH	Inclination of the right orbit versus TH	1.8	1.1	<0.001	
		$os_l - or_l$ vs TH	Inclination of the left orbit versus TH	1.1	1.1	0.010	
Sagittal		$sl - n - sn$	Maxillary prominence	0.4	0.7	0.247	
		$prn - n - sn$	Nasal convexity	0.4	0.8	0.151	
		$n - prn - sn$	Nasal tip angle	-0.2	1.1	0.699	
		$prn - sn - ls$	Nasolabial angle	-0.2	1.2	0.685	
		$li - sl - pg$	Mentolabial angle	0.4	1.1	0.300	

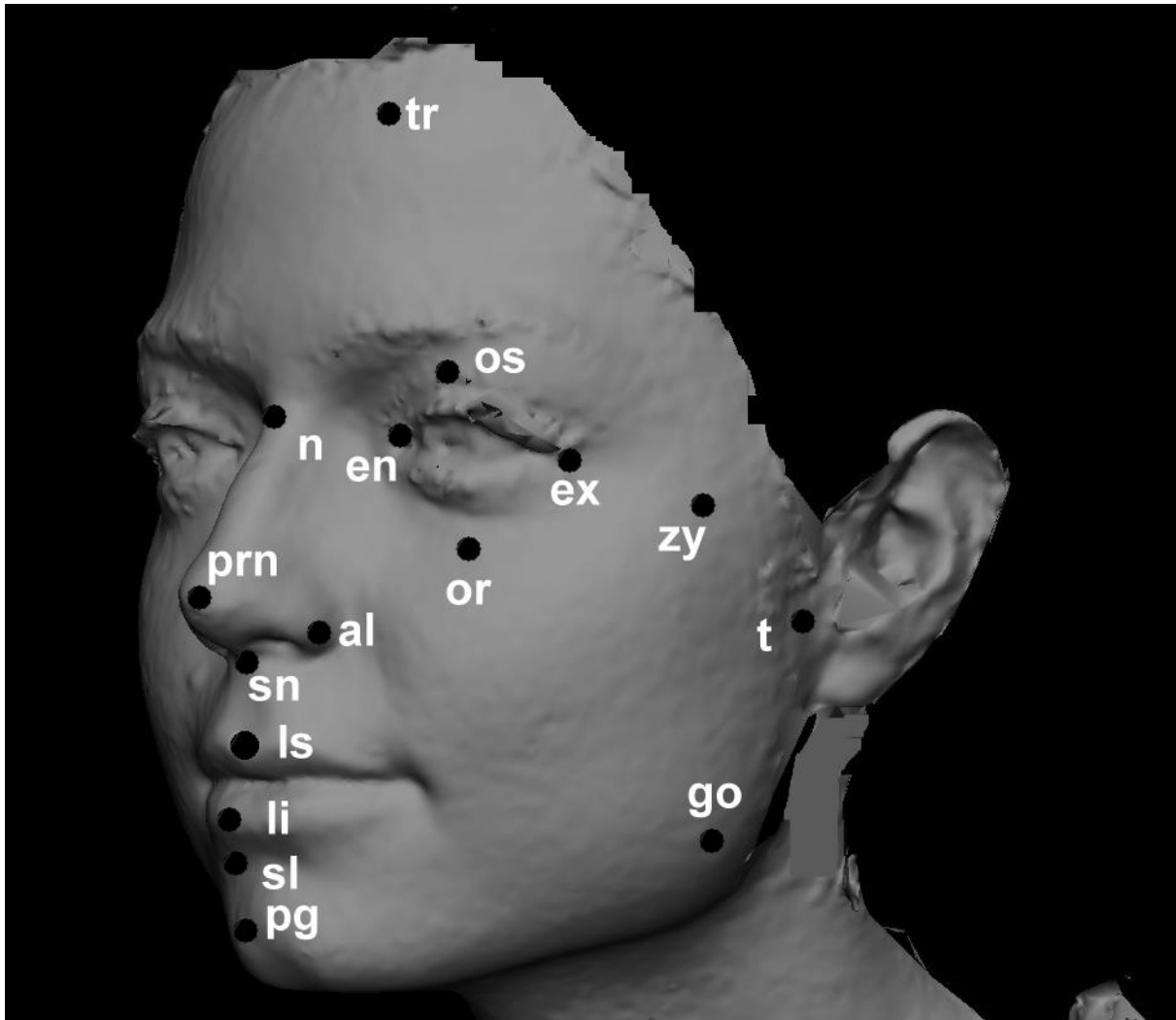
TH: true horizontal

Table 2. Facial morphological features observed in the current group of patients with AIC (data are number of patients out of 11)

Morphological features	Minimal/			Notes
	Yes	unclear	No	
sparse lateral eyebrows †	5	2	4	
prominent premaxilla †	1	1	7	relatively to a small chin 2
upturned nasal tip †	3	5	3	
upturned upper lip	3	0	8	
contracted/ reduced lower lip/ chin	3	0	8	
closed mouth	2	2	7	During the 3D photo

† According to Sutton et al. (2005)

Figure 1: Facial landmarks used for the automatic calculation of distances and angles. Unpaired (midline): t, trichion; n, nasion; prn, pronasale; sn, subnasale; ls, labiale superior; li, labiale inferior; sl, sublabiale; pg, pogonion; paired (left and right side): ex, exocanthion; en, endocanthion; os, orbitale superior; or, orbitale; al, alare; t, tragus; zy, zygion; go, gonion.



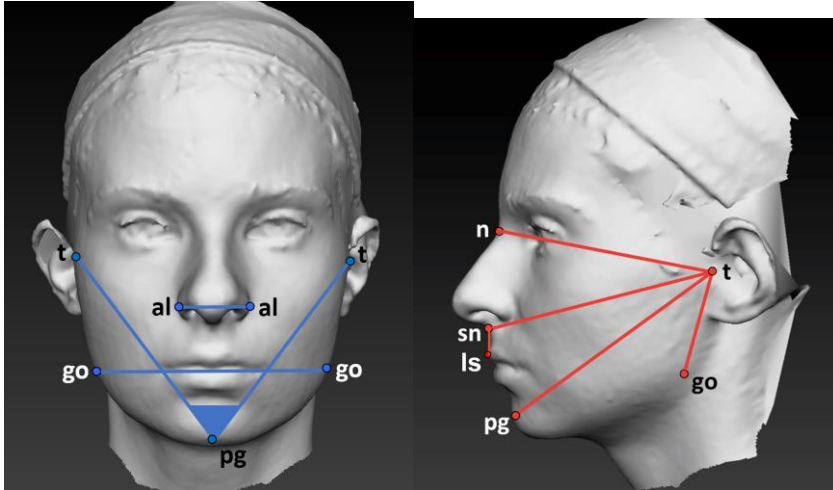


Figure 2a,b: Measurements showing statistically significant differences between patients and healthy subjects: red lines show linear distances that are smaller in patients than in healthy subjects, blue lines show linear distances that are longer in patients than in healthy subjects (only distances that differ more than ± 1 z-score are depicted). The blue triangle shows the only sagittal plane angle larger than 2 z-scores.